JOURNAL OF VIROLOGY, July 2003, p. 7611–7622 Vol. 77, No. 13
0022-538X/03/$08.00+0 DOI: 10.1128/JVI.77.13.7611–7622.2003

Molecular Distinction between Pathogenic and Infectious Properties of the Prion Protein

Roberto Chiesa,[1,2] Pedro Piccardo,[3]† Elena Quaglio,[1]‡ Bettina Drisaldi,[1]§ San Ling Si-Hoe,[1] Masaki Takao,[3]‖ Bernardino Ghetti,[3] and David A. Harris[1]*

Department of Cell Biology and Physiology, Washington University School of Medicine, St. Louis, Missouri 63110[1]; Dulbecco Telethon Institute and Department of Neuroscience, Istituto di Ricerche Farmacologiche "Mario Negri," Milan 20157, Italy[2]; and Division of Neuropathology, Indiana University School of Medicine, Indianapolis, Indiana 46202[3]

Received 8 January 2003/Accepted 2 April 2003

Tg(PG14) mice express a prion protein (PrP) with a nine-octapeptide insertion associated with a human familial prion disease. These animals spontaneously develop a fatal neurodegenerative disorder characterized by ataxia, neuronal apoptosis, and accumulation in the brain of an aggregated and weakly protease-resistant form of mutant PrP (designated $PG14^{spon}$). Brain homogenates from Tg(PG14) mice fail to transmit disease after intracerebral inoculation into recipient mice, indicating that $PG14^{spon}$, although pathogenic, is distinct from PrP^{Sc}, the infectious form of PrP. In contrast, inoculation of Tg(PG14) mice with exogenous prions of the RML strain induces accumulation of $PG14^{RML}$, a PrP^{Sc} form of the mutant protein that is infectious and highly protease resistant. Like PrP^{Sc}, both $PG14^{spon}$ and $PG14^{RML}$ display conformationally masked epitopes in the central and octapeptide repeat regions. However, these two forms differ profoundly in their oligomeric states, with $PG14^{RML}$ aggregates being much larger and more resistant to dissociation. Our analysis provides new molecular insight into an emerging puzzle in prion biology, the discrepancy between the infectious and neurotoxic properties of PrP.

Prion diseases, or transmissible spongiform encephalopathies, are fatal neurodegenerative disorders that exist in sporadic, familial, and infectiously acquired forms. There is now considerable evidence that these diseases are caused by conformational conversion of the cellular prion protein PrP^{C}, a membrane glycoprotein of uncertain function, into PrP^{Sc}, a β-rich and protease-resistant isoform that appears to be infectious in the absence of nucleic acid (11, 35). Although considerable effort has been expended during the past 20 years to define the chemical nature of prions, a major gap exists in our understanding of how prion propagation kills neurons (8). Present evidence indicates that neuronal damage is not due to loss of the normal function of PrP^{C} upon its conversion to PrP^{Sc} but rather to a toxic effect of PrP^{Sc} or some other abnormal form of PrP generated during the conversion process (4, 27, 28). However, the identities of the neurotoxic species and the nature of the cellular pathways that are activated leading to neuronal death remain obscure.

It has commonly been assumed that PrP^{Sc} itself is the primary cause of neurodegeneration in prion diseases, based on the temporal and anatomical correlation between the accumulation of this form and the development of neuropathological changes. However, there are a number of situations where this correlation is weak or absent (reviewed in reference 8). In several kinds of transmission experiments, for example, significant pathology and/or clinical dysfunction develops with little accumulation of PrP^{Sc} (14, 23, 29). In addition, some familial prion diseases are not transmissible and are not accompanied by the accumulation of protease-resistant PrP (2, 34, 43–45). The same is true for the spontaneous neurodegenerative illnesses exhibited by several kinds of PrP-transgenic mice (16, 30, 38, 39, 41, 51). On the other hand, there are subclinical infections in which there is abundant PrP^{Sc} but little symptomatology, for example, after inoculation of hamster prions into mice (18, 36).

Taken together, these situations argue that PrP^{Sc}, the infectious form of PrP, is not always the proximate cause of neuronal dysfunction and degeneration in prion diseases. Thus, alternative forms of PrP, distinct from both PrP^{C} and PrP^{Sc}, may be the primary neurotoxic species in some prion diseases. ^{Ctm}PrP, a transmembrane form of PrP, has been postulated to be one such candidate (17). Cytoplasmic PrP, which has recently been shown to be toxic in cultured cells and transgenic mice, represents another potential candidate (25, 26). As yet, however, there are few clues to the structural differences between infectious and pathogenic versions of PrP.

Tg(PG14) mice (10) provide a unique opportunity to approach this issue. These mice carry a transgene encoding the murine homologue of a nine-octapeptide insertion associated with a familial prion disease in humans (13, 22, 31). Tg(PG14) mice spontaneously develop a fatal neurological illness that recapitulates several key features of human prion disorders, including ataxia, neuronal loss, synapse-like deposition of PrP, and astrogliosis (7, 9, 10). The development of clinical symptoms and neuropathological changes correlates closely with the accumulation of an aggregated and protease-resistant form of PG14 PrP. This mutant protein resembles PrP^{Sc} in its biochemical properties with one important exception: it is ~20 to 50

* Corresponding author. Mailing address: Department of Cell Biology and Physiology, Washington University School of Medicine, 660 S. Euclid Ave., St. Louis, MO 63110. Phone: (314) 362-4690. Fax: (314) 747-0940. E-mail: dharris@cellbio.wustl.edu.

† Present address: Center for Biologics Evaluation and Research, Food and Drug Administration, Rockville, MD 20852.

‡ Present address: Istituto di Ricerche Farmacologiche "Mario Negri," 20157 Milan, Italy.

§ Present address: Center for Research in Neurodegenerative Diseases, University of Toronto, Toronto, Ontario M5S 3H2, Canada.

‖ Present address: Department of Neurology, School of Medicine, Keio University, Shinjyuku-ku, Tokyo 160-8582, Japan.

times less protease resistant than the PrP^{Sc} associated with most standard prion strains (10). This difference in protease resistance raises the possibility that Tg(PG14) mice harbor an unusual form of PrP that is highly pathogenic but that is structurally and biologically distinct from PrP^{Sc}. In the present paper, we explore the molecular relationship between PG14 PrP and infectious PrP^{Sc}.

MATERIALS AND METHODS

Mice. The production of transgenic mice expressing wild-type and PG14 mouse PrPs tagged with an epitope for the monoclonal antibody 3F4 has been reported previously (10). Experiments were performed on the following lines of mice: Tg(PG14) A1, A2, A3, and C (hemizygous for the transgene array unless otherwise indicated); Tg(WT) E1 (homozygous unless otherwise indicated), E3 (hemizygous), and E4 (hemizygous). All transgenic mice used in this study had been bred onto a C57BL/6J × 129/*Prn-p*$^{-/-}$ background (4) except for several of those listed as the sources of inocula in Table 1, which were on a C57BL/6J × 129/*Prn-p*$^{+/+}$ background. CD1 mice were obtained from Charles River Laboratories (Wilmington, Mass.).

Transmission studies. Ten percent (wt/vol) homogenates of mouse brain were prepared in phosphate-buffered saline using sterile, disposable tissue grinders. After being cleared by centrifugation at 900 × *g* for 5 min, the homogenates were diluted to a final concentration of 1 or 2.5% in phosphate-buffered saline, and 25 μl was injected intracerebrally into the right parietal lobes of 4- to 6-week-old recipient mice using a 25-gauge needle. To monitor the appearance and development of neurological symptoms, the mice were scored according to a set of objective criteria (10). The RML isolate of scrapie (6) was obtained from Byron Caughey and Richard Race (Rocky Mountain Laboratories) and was passaged repeatedly in CD1 mice.

PK resistance. Proteinase K (PK) resistance assays were carried out as described previously (10) using brain lysates (1 mg of protein/ml) prepared in HB (10 mM Tris-HCl [pH 7.4], 100 mM NaCl, 0.5% Nonidet P-40, 0.5% sodium deoxycholate). In some experiments, PK-digested samples were deglycosylated with *N*-glycosidase F (0.01 U/ml; New England Biolabs) for 16 h at 37°C prior to sodium dodecyl sulfate-polyacrylamide gel electrophoresis (SDS-PAGE).

Conformation-dependent immunoassay of PrP. Brain lysates were diluted to 0.25 mg/ml in HB containing protease inhibitors (pepstatin and leupeptin, 1 μg/ml; phenylmethylsulfonyl fluoride, 0.5 mM; and EDTA, 2 mM) and incubated for 20 min at 4°C. After a brief centrifugation to remove debris, samples were divided into two aliquots. SDS (1% final concentration) was added to one of the aliquots, which was then incubated at 95°C for 10 min. After the addition of Nonidet P-40 (1% final concentration), both aliquots were precleared with *Staphylococcus* (Pansorbin; Calbiochem) for 1 h at 4°C, and PrP was immunoprecipitated using the antibody 3F4 or P45-66 and collected on protein A-Sepharose beads. The immunoprecipitated PrP was released from the beads with SDS-PAGE sample buffer and analyzed by immunoblotting using biotinylated 3F4 antibody and horseradish peroxidase-streptavidin. Films exposed by enhanced chemiluminescence (Amersham) were digitized with an Epson Expression 636 scanner, and PrP band intensities were quantitated by SigmaScan Image (Jandel Scientific).

Sedimentation of PrP in sucrose gradients. The brain lysates were diluted to a final concentration of 0.25 mg/ml (total protein) in HB supplemented with protease inhibitors, incubated for 20 min at 4°C, and centrifuged at 16,000 × *g* for 5 min; 0.5 ml of the cleared samples was fractionated on a 5-ml linear gradient of sucrose in HB by centrifugation at 4°C in an MLS-55 rotor using an Optima MAX-E ultracentrifuge (Beckman). After centrifugation, 0.5-ml fractions of the gradient and the pellet were collected, and proteins in each fraction were methanol precipitated and analyzed by Western blotting using the 3F4 antibody. In some experiments, samples were incubated with PK (0.5 to 20 μg/ml) before methanol precipitation. Sedimentation markers run in parallel gradients included carbonic anhydrase (29 kDa; 3.2S), bovine serum albumin (65 kDa; 4.6S), aldolase (158 kDa; 7.4S), catalase (232 kDa; 11.3S), and ferritin (440 kDa; 16.6S).

Urea-induced disaggregation of PrP. Brain lysates were diluted in TND (20 mM Tris-HCl [pH 7.4], 0.5% Nonidet P-40, and 0.5% sodium deoxycholate) to a protein concentration of 0.3 mg/ml, incubated for 20 min at 4°C, and cleared by centrifugation at 16,000 × *g* for 5 min; 0.15 ml of 2× urea in TND buffer was added to 0.15 ml of the cleared lysates to achieve the appropriate urea concentration. Samples were incubated for 1 h at 37°C and then centrifuged at 4°C for 45 min at 186,000 × *g* in a TLA 55 rotor using an Optima MAX-E ultracentrifuge. PrP in the supernatant and pellet fractions was visualized by Western blotting using the 3F4 antibody.

Histology. Preparation of sections and immunohistochemical staining using the 3F4 antibody was carried out as described previously (10).

RESULTS

The brains of spontaneously ill Tg(PG14) mice do not contain detectable infectivity. To test whether infectious prions were generated de novo in the brains of Tg(PG14) mice, nine different brain homogenates were prepared from mice of the A1, A2, or A3 line (10) that had been culled at different times after spontaneous development of clinical symptoms. These homogenates were inoculated intracerebrally into three different hosts: nontransgenic CD1 mice, Tg(WT-E1$^{+/+}$) mice that overexpress wild-type PrP carrying an epitope tag for the antibody 3F4, and Tg(PG14-C$^{+/-}$) mice that express low levels of 3F4-tagged PG14 PrP and that do not become sick spontaneously (Table 1). The PrP expressed by the latter mice should be a particularly efficient substrate for assaying infectivity, because it has the same amino acid sequence as the PrP present in the Tg(PG14) inocula. All transgenic mice used in this study carried two disrupted alleles of the *Prn-p* gene and so did not synthesize endogenous PrP. Negative control inocula included brain homogenates from nontransgenic C57BL/6J × CBA/J/*Prn-p*$^{+/+}$ mice and from Tg(WT) mice of the E1, E3, and E4 lines, which express different levels of wild-type PrP and remain healthy throughout their lives. As positive controls, some host mice of each genotype were inoculated with the mouse-adapted RML isolate of scrapie that had been previously passaged in either CD1 or Tg(WT-E1$^{+/-}$) mice. All the inoculated mice were observed on a weekly basis for the appearance of neurological symptoms, and test mice from each group were culled at several time intervals after inoculation (102 to 169, 387 to 450, and 500 to 727 days) for biochemical analysis.

None of the animals inoculated with brain homogenates from Tg(PG14) mice, or from negative control mice, developed signs of neurological dysfunction, and all the animals either died due to intercurrent illness or were sacrificed near the end of their normal life span, ~2 years after inoculation (Table 1, lines 2 to 15, 18 to 31, and 35 to 48). Moreover, none of the brains from inoculated CD1 or Tg(WT-E1$^{+/+}$) host mice that were subjected to biochemical analysis contained PrP that was detergent insoluble or that was resistant to even low concentrations (1 to 5 μg/ml) of PK (data not shown). Tg(PG14-C$^{+/-}$) mice spontaneously accumulate small amounts of detergent-insoluble, weakly PK-resistant PrP in their brains as they age (10), but inoculation with Tg(PG14) brain homogenates did not increase the amount of this protein (not shown). In contrast, all positive control mice inoculated with RML prions developed scrapie, with an incubation period that varied between 128 and 555 days, depending, as expected, on the PrP expression level and whether the inoculated PrP^{Sc} and recipient PrP^{C} both contained the 3F4 epitope tag (Table 1, lines 16, 32, 33, 49, and 50). The brains of all the scrapie-affected control mice contained PrP that was resistant to high concentrations (100 μg/ml) of PK (not shown). These data demonstrate that Tg(PG14) mice do not spontaneously generate detectable levels of infectious prions in their brains, indicating that PG14 PrP from these animals is distinct from PrP^{Sc} in its transmission properties.

Inoculation of Tg(PG14) mice with RML prions causes scrapie. We next investigated whether a different form of PG14

TABLE 1. Transmission assay for the presence of infectivity in the brains of spontaneously ill Tg(PG14) mice

Recipient[a]	Line no.	Inoculum[b]	Time to symptoms[c] (mean no. of days ± SEM)	Time to death[d] (mean no. of days ± SEM)	No. dead/total
CD1	1	None	>640		0/5
	2	Tg(PG14-A1$^{+/-}$)	>640		0/8
	3	Tg(PG14-A2$^{+/-}$)	>640		0/7
	4	Tg(PG14-A2$^{+/-}$)	>615		0/6
	5	Tg(PG14-A2$^{+/-}$)/*Prn-p*$^{-/-}$	>640		0/6
	6	Tg(PG14-A2$^{+/+}$)/*Prn-p*$^{-/-}$	>640		0/6
	7	Tg(PG14-A3$^{+/-}$)	>615		0/7
	8	Tg(PG14-A3$^{+/-}$)	>500		0/6
	9	Tg(PG14-A3$^{+/+}$)/*Prn-p*$^{-/-}$	>595		0/7
	10	Tg(PG14-A3$^{+/+}$)/*Prn-p*$^{-/-}$	>630		0/7
	11	Tg(WT-E1$^{+/-}$)/*Prn-p*$^{-/-}$	>640		0/9
	12	Tg(WT-E3$^{+/-}$)	>550		0/7
	13	Tg(WT-E4$^{+/-}$)/*Prn-p*$^{-/-}$	>610		0/9
	14	Non-Tg (C57BL/6J × CBA/J)	>595		0/7
	15	Non-Tg (C57BL/6J × CBA/J)	>620		0/7
	16	RML[e]	128 ± 2	154 ± 3	15/15
Tg(WT-E1$^{+/+}$)/*Prn-p*$^{-/-}$	17	None	>540		0/4
	18	Tg(PG14-A1$^{+/-}$)	>520		0/10
	19	Tg(PG14-A2$^{+/-}$)	>515		0/6
	20	Tg(PG14-A2$^{+/-}$)	>495		0/5
	21	Tg(PG14-A2$^{+/-}$)/*Prn-p*$^{-/-}$	>515		0/2
	22	Tg(PG14-A2$^{+/+}$)/*Prn-p*$^{-/-}$	>540		0/7
	23	Tg(PG14-A3$^{+/-}$)	>530		0/5
	24	Tg(PG14-A3$^{+/-}$)	>515		0/8
	25	Tg(PG14-A3$^{+/+}$)/*Prn-p*$^{-/-}$	>540		0/6
	26	Tg(PG14-A3$^{+/+}$)/*Prn-p*$^{-/-}$	>515		0/8
	27	Tg(WT-E1$^{+/-}$)/*Prn-p*$^{-/-}$	>495		0/9
	28	Tg(WT-E3$^{+/-}$)	>485		0/10
	29	Tg(WT-E4$^{+/-}$)/*Prn-p*$^{-/-}$	>485		0/7
	30	Non-Tg (C57BL/6J × CBA/J)	>515		0/8
	31	Non-Tg (C57BL/6J × CBA/J)	>530		0/9
	32	RML[e]	217 ± 11	251 ± 26	4/4
	33	RML → WT(E1)[f]	183 ± 4	202 ± 4	5/5
Tg(PG14-C$^{+/-}$)/*Prn-p*$^{-/-}$	34	None	>730		0/8
	35	Tg(PG14-A1$^{+/-}$)	>625		0/6
	36	Tg(PG14-A2$^{+/-}$)	>570		0/6
	37	Tg(PG14-A2$^{+/-}$)	>550		0/7
	38	Tg(PG14-A2$^{+/-}$)/*Prn-p*$^{-/-}$	>570		0/7
	39	Tg(PG14-A2$^{+/+}$)/*Prn-p*$^{-/-}$	>615		0/6
	40	Tg(PG14-A3$^{+/-}$)	>590		0/8
	41	Tg(PG14-A3$^{+/-}$)	>640		0/8
	42	Tg(PG14-A3$^{+/+}$)/*Prn-p*$^{-/-}$	>640		0/6
	43	Tg(PG14-A3$^{+/+}$)/*Prn-p*$^{-/-}$	>605		0/6
	44	Tg(WT-E1$^{+/-}$)/*Prn-p*$^{-/-}$	>590		0/6
	45	Tg(WT-E3$^{+/-}$)	>630		0/6
	46	Tg(WT-E4$^{+/-}$)/*Prn-p*$^{-/-}$	>630		0/7
	47	Non-Tg (C57BL/6J × CBA/J)	>605		0/6
	48	Non-Tg (C57BL/6J × CBA/J)	>625		0/6
	49	RML[e]	555 ± 6	624 ± 21	8/8
	50	RML → WT(E1)[f]	539 ± 21	628 ± 19	8/8

[a] Recipient mice were inoculated intracerebrally at 25 to 50 days of age.
[b] Inocula consisted of 2.5% (wt/vol) brain homogenates prepared from mice of the indicated genotypes. All Tg(PG14) mice were clinically ill at the time brain homogenates were prepared.
[c] For mice that remained healthy, the time after inoculation at which the animals were sacrificed to terminate the experiment is given. For other mice (lines 16, 32, 33, 49, and 50), the time from inoculation to onset of symptoms is given.
[d] Time from inoculation to death. Mice that died of nonneurological intercurrent illness are excluded.
[e] RML prions passaged repeatedly in CD1 mice.
[f] RML prions passaged repeatedly in CD1 mice and then once in Tg(WT-E1) mice.

PrP would be produced after inoculation of Tg(PG14) mice with infectious prions. When the RML strain was injected intracerebrally into Tg(PG14-C$^{+/-}$) mice that do not become ill spontaneously, these animals developed typical symptoms of murine scrapie, including kyphosis, ruffled coat, foot clasp reflex, abnormal gait, rigidity, and tail plasticity (Table 2, line 1). The incubation time in these mice was long (555 and 624 days, respectively, to the onset of symptoms and to death) because of

TABLE 2. Transmission of RML prions to transgenic and nontransgenic mice

Recipient[a]	PrP expression[b]	Line no.	Inoculum[c]	Time to symptoms (mean no. of days ± SEM)	Time to death (mean no. of days ± SEM)	No. dead/ total
Tg(PG14-C$^{+/-}$)/*Prn-p*$^{-/-}$	0.15×	1	RML	555 ± 6	624 ± 21	8/8
		2	RML → WT(E1)	539 ± 21	628 ± 19	8/8
Tg(PG14-C$^{+/+}$)/*Prn-p*$^{-/-}$	0.3×	3	RML	437 ± 2	489 ± 10	3/3
		4	RML → WT(E1)	384 ± 15	438 ± 2	5/5
Tg(PG14-A3$^{+/-}$)/*Prn-p*$^{-/-}$	1×	5	None	243 ± 7[d]	449 ± 17[d]	23/23
		6	RML	239 ± 28	327 ± 8	4/4
		7	RML → WT(E1)	181 ± 25	303 ± 7	4/4
		8	RML → PG14(C)	141 ± 20	283 ± 19	4/4
		9	RML → PG14(A3)	118 ± 2	292 ± 10	6/6
		10	RML → PG14(C) → PG14(A3)	109 ± 1	283 ± 13	5/5
Tg(WT-E1$^{+/+}$)/*Prn-p*$^{-/-}$	4×	11	RML → PG14(C)	185 ± 1	208 ± 3	10/10
		12	RML → PG14(A3)	130 ± 5	212 ± 9	7/7
		13	RML → PG14(C) → PG14(A3)	144 ± 3	231 ± 8	7/7
CD1	1×	14	RML → PG14(C)	152 ± 1	175 ± 5	10/10
		15	RML → PG14(A3)	137 ± 2	166 ± 3	11/12
		16	RML → PG14(C) → PG14(A3)	137 ± 2	162 ± 8	8/8

[a] Recipient mice were inoculated intracerebrally at 23 to 47 days of age.
[b] Expressed relative to the level of endogenous PrP present in nontransgenic mice.
[c] Inocula consisted of 1% (wt/vol) brain homogenates. RML prions were passaged repeatedly in CD1 mice and were then passaged once or twice in Tg(WT) or Tg(PG14) mice, as indicated.
[d] Age at onset of spontaneous illness or age at death (from reference 7).

the low expression level of the transgene (0.15×) and because of the sequence mismatch between PrP in the RML inoculum (wild type) and PrP in the recipient mice (PG14 with a 3F4 epitope tag). Accordingly, we observed shorter incubation times when the mice were homozygous for the transgene array (0.3× expression level) (Table 2, line 3) and when they were challenged with an RML inoculum that had been passaged once in Tg(WT) mice and therefore contained 3F4-tagged PrP (Table 2, lines 2 and 4).

Inoculation with RML prions also induced disease in Tg(PG14-A3$^{+/-}$)/*Prn-p*$^{-/-}$ mice that have a 1× expression level of PG14 PrP (Table 2, line 6). These mice develop a spontaneous neurological disorder even without inoculation (line 5), making it more difficult to distinguish the effect of RML infection. Nevertheless, it was apparent that the infected mice displayed symptoms that were more severe than those of their uninfected counterparts. In addition, they showed several features, including rigidity and tail plasticity, that are characteristic of murine scrapie but that were never seen in spontaneously ill mice. Although inoculated and uninoculated mice first developed symptoms at similar times (~240 days), the inoculated animals had a much more rapid clinical course and died earlier (Table 2, lines 5 and 6). The age at death for inoculated mice was 352 ± 8 days (327 ± 8 days after inoculation) compared to 449 ± 17 days for uninoculated mice. As observed for Tg(PG14-C) recipient mice, the incubation time and duration of illness were reduced when Tg(PG14-A3$^{+/-}$) mice were challenged with an RML inoculum passaged in Tg(WT) mice (Table 2, line 7).

Identification of a highly protease-resistant form of PG14 PrP. During propagation of RML prions in Tg(PG14) mice, it seemed likely that some of the PG14 PrP was being converted into a physical state that more closely resembled PrP^{Sc} and that was distinct from the one acquired by the mutant protein in spontaneously ill animals. To determine if this was the case, we compared the PK resistance of PrP in brain samples from uninoculated and RML-infected Tg(PG14) mice. We observed that the infected animals contained a population of PrP molecules that was resistant to high concentrations of PK (50 to 100 μg/ml) (Fig. 1A, lanes 5 to 8). In contrast, the PrP from spontaneously ill uninoculated Tg(PG14) mice was completely digested by PK concentrations above 2 μg/ml (Fig. 1A, lanes 1 to 4). We observed that after PK digestion, the PrP from the uninoculated animals migrated predominantly as a single band at 27 kDa (Fig. 1A, lane 2). In contrast, PrP from RML-infected animals appeared as a triplet of bands of approximately equal intensities at 27, 25, and 21 kDa, presumably representing diglycosylated, monoglycosylated, and unglycosylated PrP, respectively (Fig. 1A, lanes 6 to 8). After enzymatic deglycosylation, the PK-resistant fragments from both kinds of mice migrated as a single band at ~21 kDa (Fig. 1B). These results indicate that the PK cleavage sites for PG14 PrP from infected and uninfected mice are probably similar but that the protease-resistant fragments are differentially glycosylated. For simplicity, we will refer to the highly PK-resistant form of PG14 PrP found in RML-inoculated Tg(PG14) mice as PG14^{RML} and the weakly PK-resistant form found in uninoculated mice as PG14^{spon} (for spontaneous).

PG14^{RML} is infectious. The strong PK resistance of PG14^{RML} suggested that it represented PrP^{Sc}. To confirm this idea, we tested the infectivity of PG14^{RML} in serial-transmission experiments in which RML prions passaged once in Tg(PG14) mice were passaged a second and third time in several kinds of recipient mice. For secondary-passage experiments, we inoculated brain homogenates from RML-infected Tg(PG14-C$^{+/-}$) and Tg(PG14-A3$^{+/-}$) mice into CD1, Tg(WT-E1$^{+/+}$), and Tg(PG14-A3$^{+/-}$) host mice. All the inoculated animals developed neurological symptoms typical of scrapie (Table 2, lines 8, 9, 11, 12, 14, and 15), and all had detergent-insoluble and highly PK-resistant PrP in their brains (data not shown). For tertiary-passage experiments, RML prions were passaged twice in Tg(PG14) mice (first in the C line

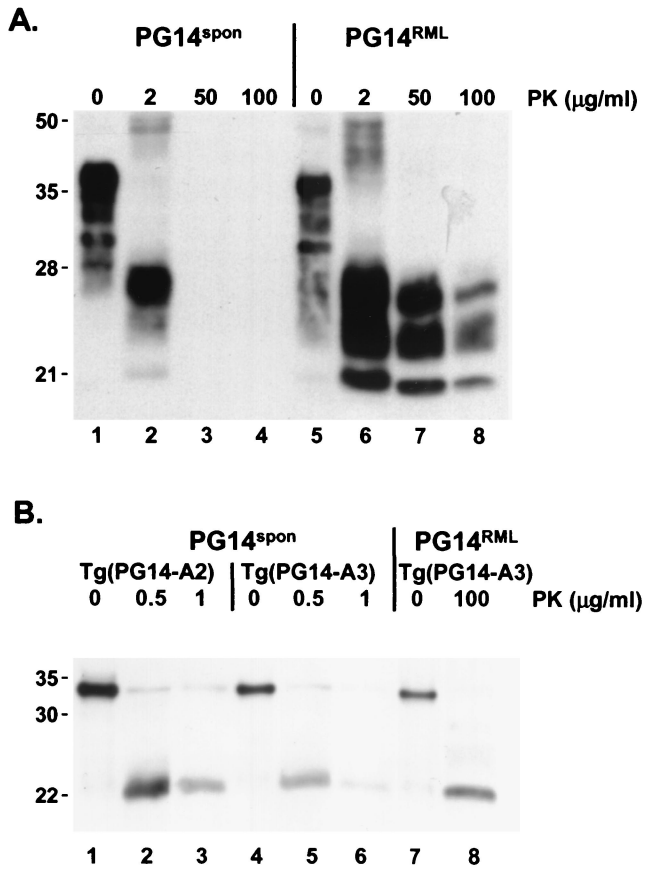

FIG. 1. PG14^{spon} and PG14^{RML} differ in protease resistance and display different patterns of glycosylation. (A) Brain lysates from a spontaneously ill Tg(PG14-A3) mouse (289 days of age) (lanes 1 to 4) and an RML-inoculated Tg(PG14-A3) mouse (ill 249 days postinoculation) (lanes 5 to 8) were incubated with 0 to 100 μg of PK/ml for 30 min at 37°C. PrP was visualized by Western blotting using the antibody 3F4. The undigested samples (0 μg of PK/ml) represent 50 μg of protein, and the other samples represent 200 μg of protein. Mass markers are given in kDa. (B) Brain lysates were prepared from the following animals: a spontaneously ill Tg(PG14-A2$^{+/+}$) mouse (221 days of age) (lanes 1 to 3), a spontaneously ill Tg(PG14-A3) mouse (279 days of age) (lanes 4 to 6), and an RML-inoculated Tg(PG14-A3) mouse (ill 303 days postinoculation) (lanes 7 and 8). The lysates were treated with PK at the indicated concentrations, and after deglycosylation with N-glycosidase F, PrP was visualized by Western blotting with the 3F4 antibody. The undigested samples (0 μg of PK/ml) represent 2 μg of protein, and the other samples represent 8 μg of protein.

and then in the A3 line) and were then inoculated into recipient mice. Again, all the recipients became ill (Table 2, lines 10, 13, and 16). The first passage of RML prions into Tg(PG14-A3$^{+/-}$) mice produced a longer incubation time than the second and third passages, reflecting adaptation of wild-type prions to the PG14 host (Table 2, compare line 6 with lines 8 to 10). Unexpectedly, CD1 mice had shorter incubation times for PG14 inocula than the two transgenic hosts, which display a better match in the PrP amino acid sequence (Table 2, lines 14 to 16). This phenomenon could reflect the outbred genetic background of CD1 mice or else a higher intrinsic conversion efficiency of PrP lacking the 3F4 epitope tag (40). Treatment of PG14^{RML} inocula with 200 μg of PK/ml did not diminish their infectivity (data not shown), implying that it is the highly protease-resistant PrP in these samples that is infectious. Taken together, our results clearly indicate that PG14^{RML} is infectious and is therefore a form of PrP^{Sc}.

PG14^{RML} and PG14^{spon} produce distinct neuropathological profiles. To compare the neuropathologies produced by the two forms of PG14 PrP, we carried out histological analysis of the brains of RML-inoculated and uninoculated Tg(PG14) mice. We have previously reported that spontaneous neurodegeneration in Tg(PG14-A3) mice is characterized by the following features (7, 10): (i) cerebellar atrophy secondary to massive apoptosis of granule cells; (ii) synapse-like deposits of PrP in the olfactory bulb, the perforant pathway of the hippocampus, and the molecular layer of the cerebellum; (iii) hypertrophy and proliferation of astrocytes in the neocortex, hippocampus, and cerebellar cortex; and (iv) absence of spongiform change and amyloid plaques. In contrast, Tg(PG14-C) mice display no histological abnormalities.

The neuropathological changes induced by RML prions were clearly distinct from those associated with spontaneous illness in Tg(PG14-A3) mice. RML-induced pathology was easiest to appreciate in Tg(PG14-C) mice because of the absence of spontaneous neurodegeneration. However, very similar neuropathological changes were produced after inoculation of Tg(PG14-A3) mice, except that in this case, the features specifically associated with the infection were superimposed on those that occurred spontaneously. One obvious abnormality seen only in RML-inoculated animals of both the C and A3 lines was spongiform degeneration, which was most prominent in the neocortex (Fig. 2A), striatum, hippocampus (Fig. 2E and F), thalamus, and colliculi. The pattern of PrP deposition in infected mice was also different from that seen in uninoculated Tg(PG14-A3) mice. The deposits had a more widespread anatomical distribution, including subpial regions of the neocortex (Fig. 2C), the end plate region of the hippocampus (Fig. 2E and F), and the molecular, Purkinje, and granule cell layers of the cerebellum (compare Fig. 2G with H). This difference in PrP distribution was also evident when a histoblotting technique (42) was used (data not shown). The character of the PrP staining was also different in infected animals, with small, punctate deposits sometimes coexisting with larger, coarser accumulations (Fig. 2F and G). As in uninoculated Tg(PG14-A3) mice, none of these deposits was fluorescent in thioflavin S preparations, indicating the absence of amyloid (data not shown). Finally, severe astrogliosis was seen in the cerebrum and cerebellum, most prominently in areas with spongiosis (not shown). Taken together, these results argue that PG14^{RML} and PG14^{spon} induce distinct pathologies.

PG14^{spon} and PG14^{RML} react similarly in a conformation-dependent immunoassay. The availability of PG14^{spon} and PG14^{RML} provided a unique opportunity to compare the molecular properties of two forms of PrP whose primary sequences were identical but whose infectivities and pathogenic effects were markedly different. The dramatically dissimilar PK susceptibilities of these two forms strongly suggested that their molecular structures were probably distinct. To investigate the possibility that PG14^{spon} and PG14^{RML} differed from each other in secondary or tertiary structure, we first analyzed these proteins by a conformation-dependent immunoassay that compares the reactivities of certain antibodies with PrP molecules

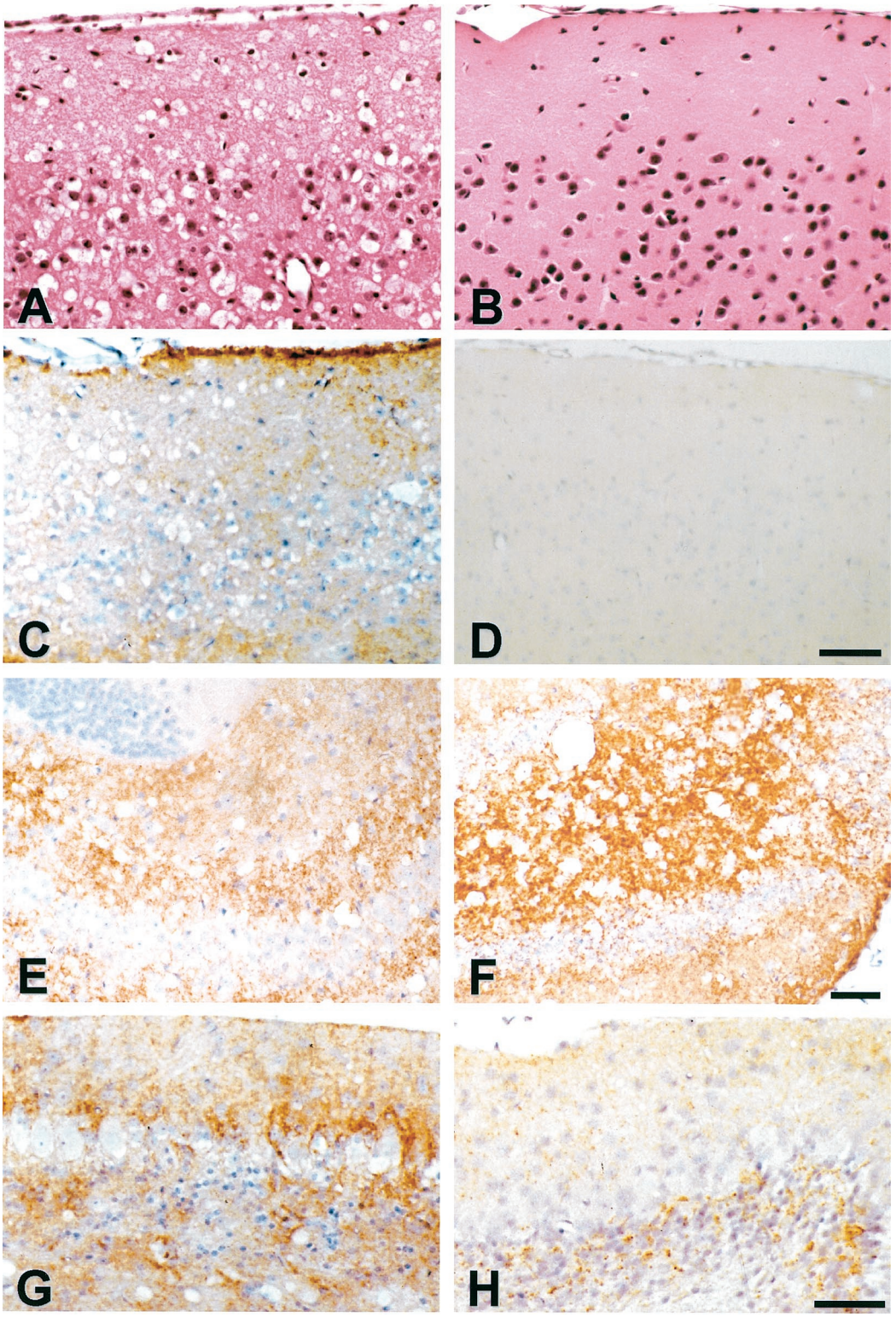

FIG. 2. Neuropathology in the cerebra and cerebella of RML-inoculated and uninoculated Tg(PG14) mice. (A) Cerebral cortex of a Tg(PG14-C) mouse inoculated with RML prions (terminally ill 586 days postinjection). There is severe spongiform degeneration. Hematoxylin-eosin stain. (B) Cerebral cortex of an uninoculated Tg(PG14-C) mouse (asymptomatic; 678 days of age). No spongiform degeneration is visible. Hematoxylin-eosin stain. (C) Cerebral cortex of the mouse shown in panel A stained with 3F4 antibody. There are numerous fine, punctate deposits of PrP in the neuropil and intense PrP accumulation beneath the leptomeninges. (D) Cerebral cortex of the mouse shown in panel B stained with 3F4 antibody. No PrP deposits are visible. (E) Hippocampus of the mouse shown in panel A stained with 3F4 antibody. The CA_4 field shows abundant fine, punctate deposits of PrP. (F) Hippocampus of a Tg(PG14-A3) mouse inoculated with RML prions (terminally ill 336 days postinjection). There are abundant coarse deposits of PrP throughout the CA_4 field. (G) Cerebellar cortex of the mouse shown in panel F stained

in the native and denatured states. This assay has been used to detect conformational variations among PrP^{Sc} molecules derived from multiple scrapie strains (37).

We utilized a modified version of the assay described by Safar et al. (37), in which PrP was immunoprecipitated with or without prior denaturation in SDS and was then analyzed by Western blotting. We employed two different antibodies: 3F4, a monoclonal antibody whose epitope (residues 108 to 111) is known to become inaccessible during the conversion of PrP^{C} to PrP^{Sc} (33), and P45-66, a polyclonal antibody that recognizes residues 45 to 66 in the octapeptide repeat region (24) and whose conformation-dependent reactivity had not been previously tested. As shown in Fig. 3A, 3F4 reacted poorly with $PG14^{spon}$ and $PG14^{RML}$ in the native state, although it efficiently immunoprecipitated the two forms of the protein after denaturation (lanes 7 to 10). Controls in this assay included PrP^{Sc} from infected hamster brain, which also reacted much better with 3F4 after denaturation (lanes 5 and 6), and hamster and mouse PrP^{C}, which reacted equally well in both the native and denatured states (lanes 1 to 4). Similar results were obtained using the antibody P45-66. $PG14^{spon}$ and $PG14^{RML}$, in contrast to PrP^{C}, reacted poorly with P45-66 in the native state (Fig. 3C). These data demonstrate that, like PrP^{Sc}, both $PG14^{spon}$ and $PG14^{RML}$ possess conformationally masked epitopes adjacent to the central hydrophobic region and within the octapeptide repeats. Quantitation of the assay data (Fig. 3B and D) showed small differences in the ratio of native and denatured immunoreactivities of $PG14^{spon}$, $PG14^{RML}$, and hamster PrP^{Sc}, suggesting that these forms have similar but possibly not identical conformations.

$PG14^{RML}$ forms larger aggregates than $PG14^{spon}$. To explain the marked difference in PK resistance between $PG14^{spon}$ and $PG14^{RML}$, we hypothesized that these forms might differ in their states of aggregation (quaternary structure). For example, $PG14^{spon}$ might form smaller oligomers than $PG14^{RML}$ or assemble into polymers with a different arrangement of subunits. To characterize the size distributions of $PG14^{spon}$ and $PG14^{RML}$ oligomers, we fractionated brain lysates from spontaneously ill and RML-inoculated Tg(PG14) mice by velocity sedimentation on sucrose gradients. In an initial series of experiments using several different centrifugation conditions, we noticed that, although there was overlap between the size distributions of PrP from infected and uninfected mice, there was consistently a larger proportion of PrP from the infected animals (~20% of the total) that sedimented with S values of >20 (data not shown).

To analyze the size distributions of these larger aggregates, we centrifuged infected brain lysates on a 25 to 50% sucrose gradient at 175,000 × *g* for 1 h and then treated the gradient fractions with 20 μg of PK/ml prior to Western blotting in order to reveal the presence of highly PK-resistant $PG14^{RML}$ forms. For comparison, we performed the same sedimentation analysis on uninfected lysates but used 1 μg of PK/ml to digest the gradient fractions in order to reveal the distribution of weakly PK-resistant $PG14^{spon}$ molecules. We observed that $PG14^{RML}$ was found throughout the lower two-thirds of the gradient (fractions 4 to 9 and the pellet) (Fig. 4A and B). We estimate that the majority of $PG14^{RML}$ aggregates have a sedimentation coefficient of >50S, with ~30% of them (those in the pellet) having a sedimentation coefficient of >120S. If composed exclusively of PrP, the latter aggregates would contain >200 molecules of the protein. In contrast, $PG14^{spon}$ was present almost entirely in fractions 1 to 3, corresponding to S values of <20S (Fig. 4A and B). In experiments using longer centrifugation runs to separate smaller molecules (not shown), we determined that 15 to 20% of $PG14^{spon}$ PrP was monomeric (3.2S), with the rest sedimenting at 16 to 20S (corresponding to oligomers containing ~20 to 30 molecules of PrP). Under these conditions, >80% of the PrP in brain lysates from Tg(WT) mice was found in the monomer fraction. These results demonstrate that $PG14^{RML}$ molecules form significantly larger aggregates than $PG14^{spon}$ molecules.

$PG14^{RML}$ aggregates are more resistant to urea-induced dissociation. To determine whether $PG14^{spon}$ and $PG14^{RML}$ oligomers differed not only in size but also in how "tightly" their subunits were associated, we assessed the susceptibilities of the two forms to disaggregation by the protein denaturant urea. Brain lysates from uninoculated and RML-infected Tg(PG14) mice were incubated with increasing concentrations of urea (1 to 4 M) for 1 h at 37°C. The samples were then centrifuged at 186,000 × *g* (a condition that pellets aggregated but not monomeric PrP), and the amounts of PG14 PrP in the supernatant and in the pellet were analyzed by Western blotting. We observed that, at all urea concentrations tested, PrP from inoculated mice was less efficiently dissociated into soluble form (Fig. 4C and D). At 3 M urea, only 5% of the PrP from uninfected mice remained aggregated compared to 30% of the protein from infected animals. Even at 4 M urea, 20% of the PrP from infected samples was still aggregated. These results indicate that a subpopulation of PrP in infected brain, representing ~20% of the total, is highly resistant to urea-induced disaggregation.

To determine whether this tightly aggregated fraction of PrP was also highly protease resistant, brain lysates were treated with 4 M urea and centrifuged at 186,000 × *g*, and the supernatant and pellet fractions were subjected to digestion with 20 μg of PK/ml. As shown in Fig. 4E, PrP recovered in the pellet after ultracentrifugation (lane 2) was fully resistant to PK digestion (lane 4), whereas the solubilized protein in the supernatant (lane 1) was degraded by the protease (lane 3). This result demonstrates that the $PG14^{RML}$ aggregates found in infected brain are more urea resistant, as well as more protease resistant, than the $PG14^{spon}$ aggregates present in uninfected brain.

DISCUSSION

Tg(PG14) mice carry a transgene encoding the murine homologue of a nine-octapeptide insertional mutation that is

with 3F4 antibody. The molecular, Purkinje, and granule cell layers show abundant PrP deposition. (H) Cerebellar cortex of an uninoculated Tg(PG14-A3$^{+/+}$) mouse (terminally ill at 183 days of age) stained with 3F4 antibody. The molecular, Purkinje, and granule cell layers show less intense PrP deposition than in the RML-inoculated mouse shown in panel G. Bars: panel D, 50 μm (same scale for panels A to C); panel F, 50 μm (same scale for panel E); and panel H, 25 μm (same scale for panel G).

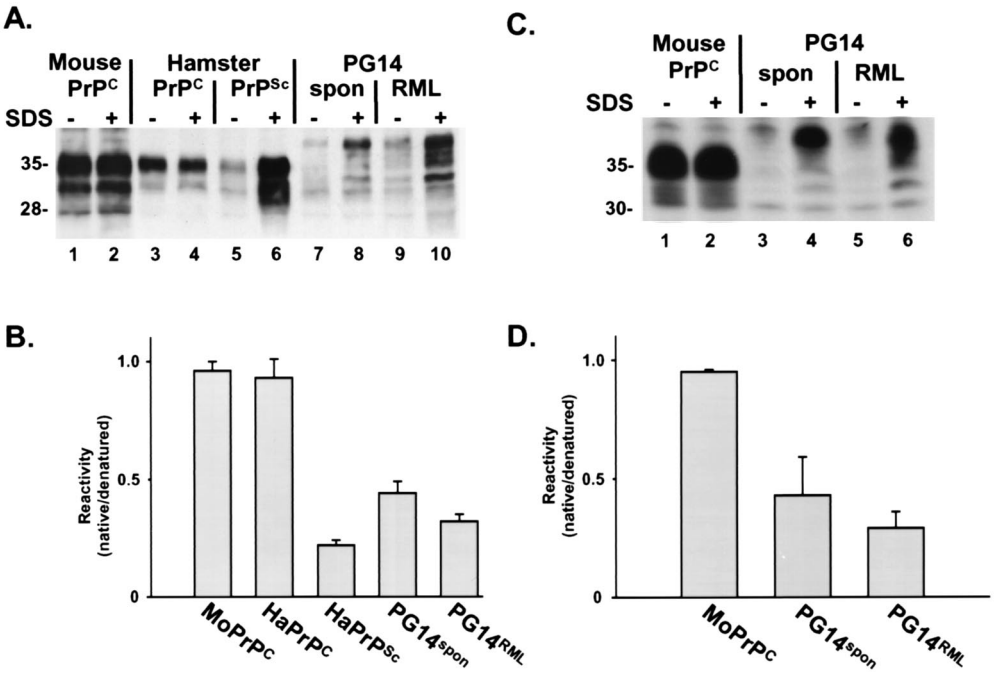

FIG. 3. PG14^{spon} and PG14^{RML} react poorly in the native state with antibodies 3F4 and P45-66. (A) Brain lysates were prepared from the following animals: an uninoculated Tg(WT-E1) mouse (lanes 1 and 2), an uninoculated hamster (lanes 3 and 4), a hamster inoculated with the 263K strain of scrapie (lanes 5 and 6), a spontaneously ill Tg(PG14-A3) mouse (289 days of age) (lanes 7 and 8), and an RML-infected Tg(PG14-A3) mouse (ill 315 days postinoculation) (lanes 9 and 10). PrP was immunoprecipitated from the lysates with antibody 3F4. Prior to immunoprecipitation, some samples (lanes 2, 4, 6, 8, and 10) were incubated at 95°C for 10 min in the presence of 1% SDS (+). The immunoprecipitated PrP was run on SDS-PAGE, immunoblotted using biotinylated 3F4, and visualized by enhanced chemiluminescence using horseradish peroxidase-streptavidin. (B) PrP was quantitated by densitometric analysis of blots such as the one shown in panel A. Reactivity with 3F4 was expressed as the ratio of PrP immunoprecipitated in the absence of SDS (native) to PrP immunoprecipitated in the presence of SDS (denatured). Each bar represents the mean plus standard error of the mean (SEM) of three to eight independent experiments. (C) Brain lysates were prepared from the following animals: an uninoculated Tg(WT-E1) mouse (lanes 1 and 2), a spontaneously ill Tg(PG14-A3) mouse (369 days old) (lanes 3 and 4), and an RML-injected Tg(PG14-A3) mouse (ill 300 days postinoculation) (lanes 5 and 6). PrP was immunoprecipitated from native lysates (lanes 1, 3, and 5) or from SDS-denatured lysates (lanes 2, 4, and 6) using the polyclonal antibody P45-66 and was immunoblotted as described for panel A. (D) PrP was quantitated from blots such as those shown in panel C and was plotted as described for panel B. Each bar represents the mean + SEM of three independent experiments.

associated with a familial prion disease in humans. In this study, we conducted a comparison of PG14^{spon} and PG14^{RML}, two different forms of mutant PrP produced in the brains of Tg(PG14) mice. These two forms have the same amino acid sequence but display markedly different biological and molecular properties (Fig. 5). PG14^{spon}, which accumulates in spontaneously ill, uninoculated mice, is weakly protease resistant and is not infectious in animal transmission experiments. In contrast, PG14^{RML}, which is produced after inoculation of Tg(PG14) mice with RML prions, is strongly protease resistant and can be serially propagated in both transgenic and nontransgenic hosts. Both forms of mutant PrP are pathogenic, but the neuropathological profiles they produce are distinct, consistent with the differences in their physical properties. Taken together, our results suggest a molecular explanation for the dissociation between the infectious and neurotoxic properties of PrP that has been observed in a growing number of situations, and they shed new light on the poorly understood issue of how prion propagation might damage neurons.

PG14^{spon} is not PrP^{Sc}. Our previous observation (10) that PG14^{spon} is 20- to 50-fold less PK resistant than most strains of PrP^{Sc} raised the possibility that the protein might display different transmission properties. Consistent with this prediction, we demonstrated here that brain homogenates from spontaneously ill Tg(PG14) mice display no detectable infectivity when inoculated into several different transgenic and nontransgenic hosts. We cannot rule out the possibility that the inocula contain low levels of infectious prions that are undetectable in our bioassays. This might occur, for example, if prions are rapidly degraded or cleared before they have a chance to initiate infection. Even if some infectivity were present, however, its effective titer must be many orders of magnitude lower than that found in brain homogenates of RML-injected Tg(PG14) mice, which serially transmit disease to all hosts examined. We therefore conclude that PG14^{spon} does not represent a unique strain of prion that is unusually protease sensitive but rather that it is a form of PrP fundamentally distinct from PrP^{Sc}. We note that although some human prion diseases due to insertional mutations have been shown to be transmissible (15), there is no published evidence of the transmissibility of cases with the nine-octapeptide insertion. The biochemical properties of PrP from the latter cases has also not been investigated.

Tg(P101L) mice express a mutant PrP whose human homologue is associated with Gerstmann-Sträussler syndrome (20, 47). Animals with supraphysiological levels of the transgene

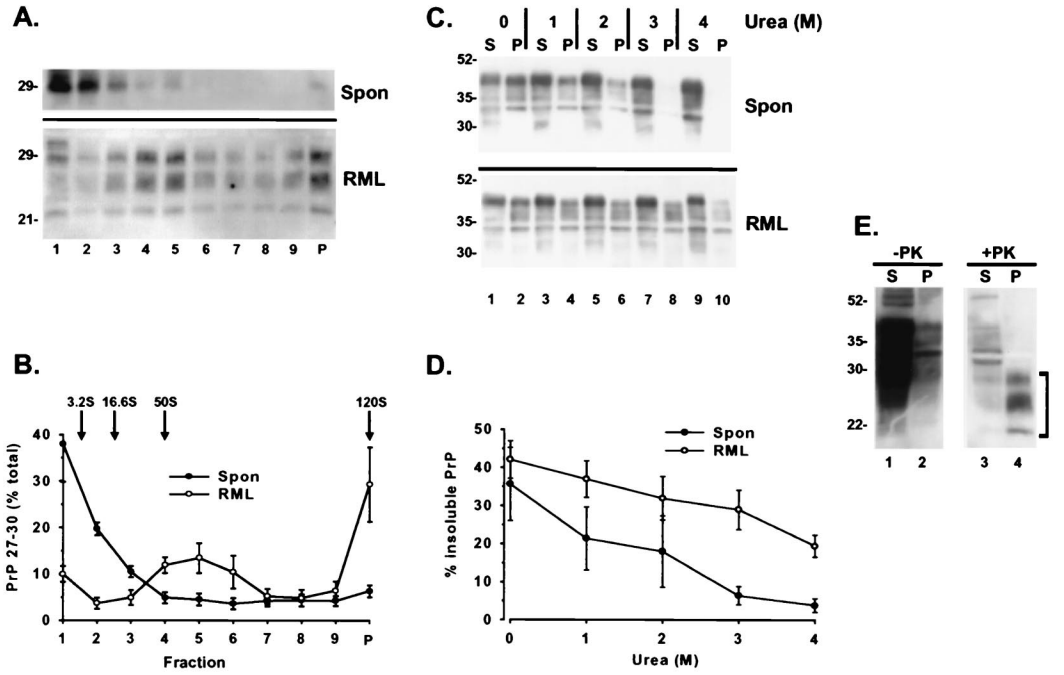

FIG. 4. PG14^{RML} aggregates are larger and more resistant to urea-induced dissociation than PG14^{spon} aggregates. (A) Brain lysates from a spontaneously ill Tg(PG14-A3) mouse (369 days of age) (top; Spon) and an RML-infected Tg(PG14-A3) mouse (ill 315 days after inoculation) (bottom; RML) were fractionated by centrifugation on a 25 to 50% sucrose gradient for 1 h at 175,000 × *g*. Fractions of the gradient (lanes 1 to 9) and the pellet (lane P) were collected and incubated with 1 (Spon) or 20 (RML) μg of PK/ml for 30 min at 37°C. PrP was then analyzed by Western blotting using the antibody 3F4. (B) The amounts of PrP 27-30 in each of the fractions of the gradient and in the pellet were quantitated by densitometric analysis of Western blots such as the ones shown in panel A and plotted as percentages of total PrP 27-30. Each point represents the mean ± standard error of the mean (SEM) of three independent experiments performed using brains from three spontaneously ill Tg(PG14) mice of the A2 and A3 lines (309 to 455 days of age) and three symptomatic Tg(PG14-A3) mice inoculated with RML prions (300 to 315 days postinoculation). The sedimentation markers run in a parallel gradient were carbonic anhydrase (3.2S) and ferritin (16.6S). The positions predicted for particles of 50 and 120S were calculated by extrapolation. (C) Detergent lysates of brains from a spontaneously ill Tg(PG14-A3$^{+/+}$) mouse (146 days of age) (top; Spon) and an RML-inoculated Tg(PG14A3) mouse (ill 315 days postinoculation) (bottom; RML) were incubated with urea at the indicated concentrations for 1 h at 37°C. Samples were then centrifuged at 168,000 × *g*, and PG14 PrP in the supernatants (S) and pellets (P) was visualized by immunoblotting it with antibody 3F4. (D) The amount of PG14 PrP in the pellet fraction after ultracentrifugation was quantitated by densitometric analysis of Western blots such as the one shown in panel C. Each point represents the mean ± SEM of four to five experiments performed with brains from four spontaneously ill Tg(PG14) mice of the A2 and A3 lines (146 to 540 days of age) and four symptomatic Tg(PG14-A3) mice inoculated with RML prions (255 and 328 days postinoculation). (E) Brain extracts from an RML-inoculated Tg(PG14-A3) mouse (ill 315 days postinoculation) were incubated with 4 M urea for 1 h at 37°C and then centrifuged at 168,000 × *g*. Supernatants (S) and pellets (P) were incubated without (lanes 1 and 2) or with (lanes 3 and 4) PK (20 μg/ml) for 30 min at 37°C. PrP was then analyzed by Western blotting using the antibody 3F4. The bracket indicates the position of PrP 27-30. The immunoreactivity in lane 3 represents a small amount of residual uncleaved PrP.

product spontaneously develop a neurodegenerative illness without protease-resistant PrP. Brain homogenates from ill Tg(P101L) mice do not transmit disease to nontransgenic mice, although they accelerate the late-onset neurodegeneration displayed by low-expressing lines of Tg(P101L) mice (19, 21, 47). It thus seems likely that P101L PrP, like PG14^{spon}, can cause significant neuropathology without being fully infectious.

PG14^{spon} and PG14^{RML} are conformationally related but differ in oligomeric state. What are the molecular differences between PG14^{spon} and PG14^{RML}, and how do these explain the profound disparity in infectivity and protease resistance between the two forms? As a probe of secondary and tertiary structures, we employed a variation of the conformation-dependent immunoassay originally developed by Safar et al. (37), which compares the accessibilities of an antibody epitope in the folded and unfolded forms of PrP. We found that, despite their dramatically different degrees of protease resistance, PG14^{spon} and PG14^{RML} behaved similarly in this assay, with epitopes in the octapeptide repeats and the central hydrophobic region being masked in the native state. The latter epitope is inaccessible in conventional strains of PrP^{Sc}, and the degree of inaccessibility has been used to classify strains (33, 37). We also observed that these two forms produced a fragment of the same size after digestion with PK, indicating that the protease was cleaving them at approximately the same site. Variations in the PK cleavage site have also been used to assay conformational differences between PrP^{Sc} strains (1, 32, 48). We conclude from these results that PG14^{spon} and PG14^{RML} PrP molecules share conformational similarities with each other and with PrP^{Sc}, at least within the central and N-terminal regions. Of course, antibody and protease accessibilities are only indirect measures of protein structure, and therefore our data do not rule out the possibility that PG14^{spon} and PG14^{RML} display subtle differences in conformation. Ulti-

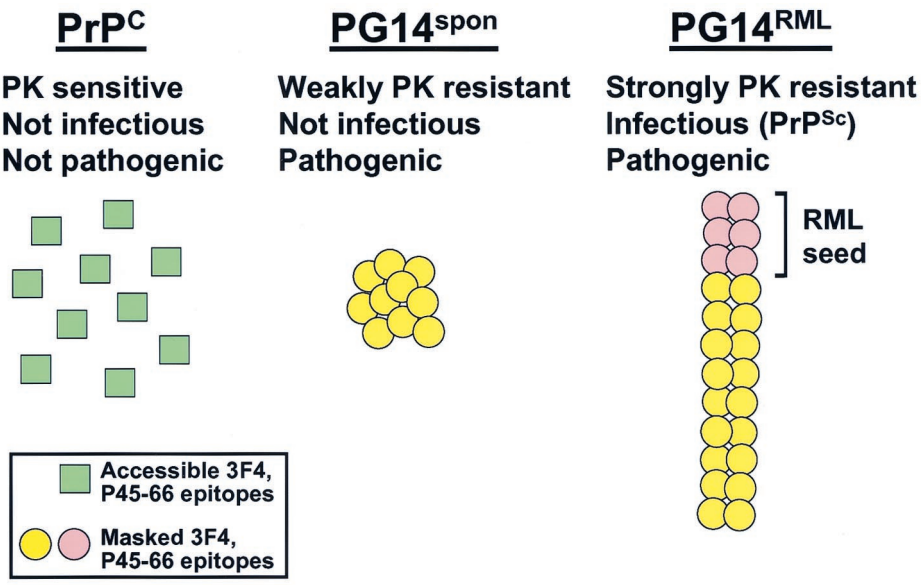

FIG. 5. Models of the structural differences between PrP^{C}, $PG14^{spon}$, and $PG14^{RML}$. See the text for an explanation.

mately, it will be necessary to purify these proteins in order to characterize their structures by biophysical techniques.

We also sought to discover differences in the oligomeric state of $PG14^{spon}$ and $PG14^{RML}$ PrP molecules. Using sucrose gradient centrifugation, we determined that the two forms differ markedly in size. Whereas most $PG14^{spon}$ aggregates had sedimentation coefficients of <20S (with ~20% being monomeric), almost all of the $PG14^{RML}$ aggregates had sedimentation coefficients of >50S. Approximately 30% of the $PG14^{RML}$ aggregates sedimented with an estimated S value of >120, approaching the size of a conventional virus. We also found that $PG14^{RML}$ aggregates were less easily dissociated by urea. After treatment with 3 to 4 M urea, a concentration that almost completely solubilized $PG14^{spon}$ oligomers, $PG14^{RML}$ aggregates remained insoluble and protease resistant. These results indicate that $PG14^{RML}$ oligomers are larger and more tightly packed than $PG14^{spon}$ oligomers. This difference in quaternary structure could readily explain the marked difference between PK resistances in the two forms, since the tightly packed PrP molecules in $PG14^{RML}$ aggregates may be less exposed to the protease (except in the region near residue 90, where both forms are cleaved).

Why is $PG14^{RML}$ infectious while $PG14^{spon}$ is not? One hypothesis is that large, tightly packed PrP oligomers are a prerequisite for prion infectivity. In this view (Fig. 5), injection of RML prions into Tg(PG14) mice would nucleate the assembly of PG14 PrP molecules into a polymer that has a size and arrangement of its subunits distinct from those exhibited by $PG14^{spon}$ oligomers, whose formation is spontaneous (not nucleated exogenously). The RML-seeded polymers could then propagate themselves upon subsequent passage, while the spontaneously generated aggregates would be incapable of seeding further polymerization. A nucleated polymerization mechanism has been demonstrated for yeast and fungal prions (49) and has been proposed for mammalian prions based on cell-free conversion experiments (5).

Neurotoxicity of PrP. In addition to highlighting the PrP structures required for prion infectivity, our results shed light on what kinds of PrP molecules are neurotoxic. A number of situations have now been recognized in which neuropathological changes develop in the apparent absence of PrP^{Sc} (for examples, see references 16, 29, and 34). Conversely, there are examples of PrP^{Sc} accumulation in the absence of neuropathological alterations or clinical symptoms (18, 36). These discrepancies have led to the growing recognition that alternative molecular forms of PrP, distinct from infectious PrP^{Sc}, may be the proximate causes of neurodegeneration in prion diseases (reviewed in reference 8). $PG14^{spon}$ is a candidate for such a pathogenic but noninfectious form of PrP.

We suggest that $PG14^{spon}$, and analogous forms of PrP carrying other disease-associated mutations, plays a prominent role in familial prion diseases. This subgroup of prion disorders is often characterized by a paucity of protease-resistant PrP^{Sc} and by a lower efficiency of transmission to laboratory animals (2, 34, 43–45). It is not difficult to rationalize the possibility that familial prion diseases involve PrP^{Sc}-independent pathogenic mechanisms, since mutations could spontaneously alter the properties of the PrP molecule in a way that makes the protein toxic but does not endow it with infectivity. Whether toxic but noninfectious forms of PrP are also generated as intermediates following exposure to exogenous prions and whether these, instead of or in addition to PrP^{Sc}, are the primary pathogenic species in these cases remain open questions.

What molecular features account for the neurotoxicity of $PG14^{spon}$? One possibility is the aggregated, conformationally altered character of this protein. There is now considerable evidence that other neurodegenerative disorders, including Alzheimer's, Parkinson's, and Huntington's diseases, are caused by accumulation of β-rich protein aggregates that are toxic to cells (46). Moreover, a number of studies suggest that small oligomers (perhaps analogous to $PG14^{spon}$), rather than highly polymerized amyloid fibrils, are the primary toxic enti-

ties in these disorders (3, 50). Whether common cytotoxic responses are triggered by protein aggregates in all of these diseases remains to be determined. PrP, unlike the proteins involved in the other neurodegenerative diseases, is membrane anchored, although recent evidence (25, 26) suggests that it can be retrotranslocated into the cytoplasm, where it is toxic. Our own data argue against such a retrotranslocation mechanism and suggest instead that mutant PrP may exert its toxic effects by virtue of its accumulation in the endoplasmic reticulum (12). Regardless of which pathway is involved, however, the data presented here suggest that infectivity may be an incidental feature of some prion diseases and may not always be directly related to the mechanism of PrP pathogenicity. The identification of PG14^{spon} as a neurotoxic species with distinct molecular properties opens the way to exploiting this and related forms as therapeutic or diagnostic targets in prion diseases.

ACKNOWLEDGMENTS

We thank Richard Kascsak for supplying 3F4 antibody, as well as Byron Caughey and Richard Race for providing the RML scrapie isolate. We also acknowledge Stefano Thellung for help with transmission studies, Cheryl Adles for maintaining the mouse colony, and Rose Richardson for assistance with histological preparations.

This work was supported by grants from the NIH to D.A.H. (NS40975) and B.G. (P30 AG10133). R.C. was supported by Telethon-Italy (139/b/bis and TCP00083) and the McDonnell Center for Cellular and Molecular Neurobiology at Washington University and by travel grants from the *Journal of Cell Science* and NATO-CNR-Italy. R.C. is an Assistant Telethon Scientist (DTI; Fondazione Telethon).

REFERENCES

1. **Bessen, R. A., and R. F. Marsh.** 1994. Distinct PrP properties suggest the molecular basis of strain variation in transmissible mink encephalopathy. J. Virol. **68:**7859–7868.
2. **Brown, P., C. J. Gibbs, P. Rodgers-Johnson, D. M. Asher, M. P. Sulima, A. Bacote, L. G. Goldfarb, and D. C. Gajdusek.** 1994. Human spongiform encephalopathy: the National Institutes of Health series of 300 cases of experimentally transmitted disease. Ann. Neurol. **35:**513–529.
3. **Bucciantini, M., E. Giannoni, F. Chiti, F. Baroni, L. Formigli, J. Zurdo, N. Taddei, G. Ramponi, C. M. Dobson, and M. Stefani.** 2002. Inherent toxicity of aggregates implies a common mechanism for protein misfolding diseases. Nature **416:**507–511.
4. **Büeler, H., M. Fischer, Y. Lang, H. Fluethmann, H.-P. Lipp, S. J. DeArmond, S. B. Prusiner, M. Aguet, and C. Weissmann.** 1992. Normal development and behavior of mice lacking the neuronal cell-surface PrP protein. Nature **356:**577–582.
5. **Caughey, B., G. J. Raymond, M. A. Callahan, C. Wong, G. S. Baron, and L. W. Xiong.** 2001. Interactions and conversions of prion protein isoforms. Adv. Protein Chem. **57:**139–169.
6. **Chandler, R. L.** 1971. Experimental transmission of scrapie to voles and Chinese hamsters. Lancet **i:**232–233.
7. **Chiesa, R., B. Drisaldi, E. Quaglio, A. Migheli, P. Piccardo, B. Ghetti, and D. A. Harris.** 2000. Accumulation of protease-resistant prion protein (PrP) and apoptosis of cerebellar granule cells in transgenic mice expressing a PrP insertional mutation. Proc. Natl. Acad. Sci. USA **97:**5574–5579.
8. **Chiesa, R., and D. A. Harris.** 2001. Prion diseases: what is the neurotoxic molecule? Neurobiol. Dis. **8:**743–763.
9. **Chiesa, R., A. Pestronk, R. E. Schmidt, W. G. Tourtellotte, B. Ghetti, P. Piccardo, and D. A. Harris.** 2001. Primary myopathy and accumulation of PrP^{Sc}-like molecules in peripheral tissues of transgenic mice expressing a prion protein insertional mutation. Neurobiol. Dis. **8:**279–288.
10. **Chiesa, R., P. Piccardo, B. Ghetti, and D. A. Harris.** 1998. Neurological illness in transgenic mice expressing a prion protein with an insertional mutation. Neuron **21:**1339–1351.
11. **Collinge, J.** 2001. Prion diseases of humans and animals: their causes and molecular basis. Annu. Rev. Neurosci. **24:**519–550.
12. **Drisaldi, B., R. S. Stewart, C. Adles, L. R. Stewart, E. Quaglio, E. Biasini, L. Fioriti, R. Chiesa, and D. A. Harris.** 2003. Mutant PrP is delayed in its exit from the endoplasmic reticulum, but neither mutant nor wild-type PrP undergoes retrotranslocation prior to proteasomal degradation. J. Biol. Chem. 10.1074/jbc.M213247200.
13. **Duchen, L. W., M. Poulter, and A. E. Harding.** 1993. Dementia associated with a 216 base pair insertion in the prion protein gene: clinical and neuropathological features. Brain **116:**555–567.
14. **Flechsig, E., D. Shmerling, I. Hegyi, A. J. Raeber, M. Fischer, A. Cozzio, C. von Mering, A. Aguzzi, and C. Weissmann.** 2000. Prion protein devoid of the octapeptide repeat region restores susceptibility to scrapie in PrP knockout mice. Neuron **27:**399–408.
15. **Goldfarb, L. G., P. Brown, W. R. McCombie, D. Goldgaber, G. D. Swergold, P. R. Wills, L. Cervenakova, H. Baron, C. J. Gibbs, Jr., and D. C. Gajdusek.** 1991. Transmissible familial Creutzfeldt-Jakob disease associated with five, seven, and eight extra octapeptide coding repeats in the PRNP gene. Proc. Natl. Acad. Sci. USA **88:**10926–10930.
16. **Hegde, R. S., J. A. Mastrianni, M. R. Scott, K. A. Defea, P. Tremblay, M. Torchia, S. J. DeArmond, S. B. Prusiner, and V. R. Lingappa.** 1998. A transmembrane form of the prion protein in neurodegenerative disease. Science **279:**827–834.
17. **Hegde, R. S., P. Tremblay, D. Groth, S. J. DeArmond, S. B. Prusiner, and V. R. Lingappa.** 1999. Transmissible and genetic prion diseases share a common pathway of neurodegeneration. Nature **402:**822–826.
18. **Hill, A. F., S. Joiner, J. Linehan, M. Desbruslais, P. L. Lantos, and J. Collinge.** 2000. Species-barrier-independent prion replication in apparently resistant species. Proc. Natl. Acad. Sci. USA **97:**10248–10253.
19. **Hsiao, K. K., D. Groth, M. Scott, S.-L. Yang, H. Serban, D. Rapp, D. Foster, M. Torchia, S. J. DeArmond, and S. B. Prusiner.** 1994. Serial transmission in rodents of neurodegeneration from transgenic mice expressing mutant prion protein. Proc. Natl. Acad. Sci. USA **91:**9126–9130.
20. **Hsiao, K. K., M. Scott, D. Foster, D. F. Groth, S. J. DeArmond, and S. B. Prusiner.** 1990. Spontaneous neurodegeneration in transgenic mice with mutant prion protein. Science **250:**1587–1590.
21. **Kaneko, K., H. L. Ball, H. Wille, H. Zhang, D. Groth, M. Torchia, P. Tremblay, J. Safar, S. B. Prusiner, S. J. DeArmond, M. A. Baldwin, and F. E. Cohen.** 2000. A synthetic peptide initiates Gerstmann-Sträussler-Scheinker (GSS) disease in transgenic mice. J. Mol. Biol. **295:**997–1007.
22. **Krasemann, S., I. Zerr, T. Weber, S. Poser, H. Kretzschmar, G. Hunsmann, and W. Bodemer.** 1995. Prion disease associated with a novel nine octapeptide repeat insertion in the PRNP gene. Mol. Brain Res. **34:**173–176.
23. **Lasmezas, C. I., J. P. Deslys, O. Robain, A. Jaegly, V. Beringue, J. M. Peyrin, J. G. Fournier, J. J. Hauw, J. Rossier, and D. Dormont.** 1997. Transmission of the BSE agent to mice in the absence of detectable abnormal prion protein. Science **275:**402–405.
24. **Lehmann, S., and D. A. Harris.** 1995. A mutant prion protein displays an aberrant membrane association when expressed in cultured cells. J. Biol. Chem. **270:**24589–24597.
25. **Ma, J., and S. Lindquist.** 2002. Conversion of PrP to a self-perpetuating PrP^{Sc}-like conformation in the cytosol. Science **298:**1785–1788.
26. **Ma, J., R. Wollmann, and S. Lindquist.** 2002. Neurotoxicity and neurodegeneration when PrP accumulates in the cytosol. Science **298:**1781–1785.
27. **Mallucci, G. R., S. Ratte, E. A. Asante, J. Linehan, I. Gowland, J. G. Jefferys, and J. Collinge.** 2002. Post-natal knockout of prion protein alters hippocampal CA1 properties, but does not result in neurodegeneration. EMBO J. **21:**202–210.
28. **Manson, J. C., A. R. Clarke, M. L. Hooper, L. Aitchison, I. McConnell, and J. Hope.** 1994. 129/Ola mice carrying a null mutation in PrP that abolishes mRNA production are developmentally normal. Mol. Neurobiol. **8:**121–127.
29. **Manson, J. C., E. Jamieson, H. Baybutt, N. L. Tuzi, R. Barron, I. McConnell, R. Somerville, J. Ironside, R. Will, M. S. Sy, D. W. Melton, J. Hope, and C. Bostock.** 1999. A single amino acid alteration (101L) introduced into murine PrP dramatically alters incubation time of transmissible spongiform encephalopathy. EMBO J. **18:**6855–6864.
30. **Muramoto, T., S. J. DeArmond, M. Scott, G. C. Telling, F. E. Cohen, and S. B. Prusiner.** 1997. Heritable disorder resembling neuronal storage disease in mice expressing prion protein with deletion of an α-helix. Nat. Med. **3:**750–755.
31. **Owen, F., M. Poulter, J. Collinge, M. Leach, R. Lofthouse, T. J. Crow, and A. E. Harding.** 1992. A dementing illness associated with a novel insertion in the prion protein gene. Mol. Brain Res. **13:**155–157.
32. **Parchi, P., A. Giese, S. Capellari, P. Brown, W. Schulz-Schaeffer, O. Windl, I. Zerr, H. Budka, N. Kopp, P. Piccardo, S. Poser, A. Rojiani, N. Streichemberger, J. Julien, C. Vital, B. Ghetti, P. Gambetti, and H. Kretzschmar.** 1999. Classification of sporadic Creutzfeldt-Jakob disease based on molecular and phenotypic analysis of 300 subjects. Ann. Neurol. **46:**224–233.
33. **Peretz, D., R. A. Williamson, Y. Matsunaga, H. Serban, C. Pinilla, R. B. Bastidas, R. Rozenshteyn, T. L. James, R. A. Houghten, F. E. Cohen, S. B. Prusiner, and D. R. Burton.** 1997. A conformational transition at the N terminus of the prion protein features in formation of the scrapie isoform. J. Mol. Biol. **273:**614–622.
34. **Piccardo, P., J. J. Liepnieks, A. William, S. R. Dlouhy, M. R. Farlow, K. Young, D. Nochlin, T. D. Bird, R. R. Nixon, M. J. Ball, C. DeCarli, O. Bugiani, F. Tagliavini, M. D. Benson, and B. Ghetti.** 2001. Prion proteins with different conformations accumulate in Gerstmann-Sträussler-Scheinker disease caused by A117V and F198S mutations. Am. J. Pathol. **158:**2201–2207.
35. **Prusiner, S. B.** 1998. Prions. Proc. Natl. Acad. Sci. USA **95:**13363–13383.

36. **Race, R., A. Raines, G. J. Raymond, B. Caughey, and B. Chesebro.** 2001. Long-term subclinical carrier state precedes scrapie replication and adaptation in a resistant species: analogies to bovine spongiform encephalopathy and variant Creutzfeldt-Jakob disease in humans. J. Virol. **75:**10106–10112.
37. **Safar, J., H. Wille, V. Itrri, D. Groth, H. Serban, M. Torchia, F. E. Cohen, and S. B. Prusiner.** 1998. Eight prion strains have PrP^{Sc} molecules with different conformations. Nat. Med. **4:**1157–1165.
38. **Shmerling, D., I. Hegyi, M. Fischer, T. Blättler, S. Brandner, J. Götz, T. Rülicke, E. Flechsig, A. Cozzio, C. von Mering, C. Hangartner, A. Aguzzi, and C. Weissmann.** 1998. Expression of amino-terminally truncated PrP in the mouse leading to ataxia and specific cerebellar lesions. Cell **93:**203–214.
39. **Supattapone, S., E. Bouzamondo, H. L. Ball, H. Wille, H. O. Nguyen, F. E. Cohen, S. J. DeArmond, S. B. Prusiner, and M. Scott.** 2001. A protease-resistant 61-residue prion peptide causes neurodegeneration in transgenic mice. Mol. Cell. Biol. **21:**2608–2616.
40. **Supattapone, S., T. Muramoto, G. Legname, I. Mehlhorn, F. E. Cohen, S. J. DeArmond, S. B. Prusiner, and M. R. Scott.** 2001. Identification of two prion protein regions that modify scrapie incubation time. J. Virol. **75:**1408–1413.
41. **Supattapone, S., H. O. Nguyen, T. Muramoto, F. E. Cohen, S. J. DeArmond, S. B. Prusiner, and M. Scott.** 2000. Affinity-tagged miniprion derivatives spontaneously adopt protease-resistant conformations. J. Virol. **74:**11928–11934.
42. **Taraboulos, A., K. Jendroska, D. Serban, S.-L. Yang, S. J. DeArmond, and S. B. Prusiner.** 1992. Regional mapping of prion proteins in brain. Proc. Natl. Acad. Sci. USA **89:**7620–7624.
43. **Tateishi, J., and T. Kitamoto.** 1995. Inherited prion diseases and transmission to rodents. Brain Pathol. **5:**53–59.
44. **Tateishi, J., T. Kitamoto, K. Doh-Ura, Y. Sakaki, G. Steinmetz, C. Tranchant, J. M. Warter, and N. Heldt.** 1990. Immunochemical, molecular genetic, and transmission studies on a case of Gerstmann-Sträussler-Scheinker syndrome. Neurology **40:**1578–1581.
45. **Tateishi, J., T. Kitamoto, M. Z. Hoque, and H. Furukawa.** 1996. Experimental transmission of Creutzfeldt-Jakob disease and related diseases to rodents. Neurology **46:**532–537.
46. **Taylor, J. P., J. Hardy, and K. H. Fischbeck.** 2002. Toxic proteins in neurodegenerative disease. Science **296:**1991–1995.
47. **Telling, G. C., T. Haga, M. Torchia, P. Tremblay, S. J. DeArmond, and S. B. Prusiner.** 1996. Interactions between wild-type and mutant prion proteins modulate neurodegeneration in transgenic mice. Genes Dev. **10:**1736–1750.
48. **Telling, G. C., P. Parchi, S. J. DeArmond, P. Cortelli, P. Montagna, R. Gabizon, J. Mastriani, E. Lugaresi, P. Gambetti, and S. B. Prusiner.** 1996. Evidence for the formation of the pathologic isoform of the prion protein enciphering and propagating prion diversity. Science **274:**2079–2082.
49. **Uptain, S. M., and S. Lindquist.** 2002. Prions as protein-based genetic elements. Annu. Rev. Microbiol. **56:**703–741.
50. **Walsh, D. M., I. Klyubin, J. V. Fadeeva, W. K. Cullen, R. Anwyl, M. S. Wolfe, M. J. Rowan, and D. J. Selkoe.** 2002. Naturally secreted oligomers of amyloid beta protein potently inhibit hippocampal long-term potentiation *in vivo*. Nature **416:**535–539.
51. **Westaway, D., S. J. DeArmond, J. Cayetano-Canlas, D. Groth, D. Foster, S.-L. Yang, M. Torchia, G. A. Carlson, and S. B. Prusiner.** 1994. Degeneration of skeletal muscle, peripheral nerves, and the central nervous system in transgenic mice overexpressing wild-type prion proteins. Cell **76:**117–129.